

# Progress in Fundamental Pulsed Plasma Thruster Research

IEPC-2017-140

*Presented at the 35th International Electric Propulsion Conference  
Georgia Institute of Technology • Atlanta, Georgia • USA  
October 8 – 12, 2017*

William Yeong Liang Ling<sup>1</sup>  
*Beijing Institute of Technology, School of Aerospace Engineering, Beijing, 100081, China*

Zhe Zhang<sup>2</sup> and Haibin Tang<sup>3</sup>  
*Beihang University, School of Astronautics, Beijing, 100081, China*

**Abstract:** Pulsed plasma thrusters (PPTs) are a structurally simple form of electric propulsion. This simplicity lends itself well to scalability for small satellites in the kilogram weight range. However, while the structural design of PPTs may be simple, the simplicity is contrasted by the complex phenomena behind the operation of a PPT. Fundamental information regarding the plasma plume of a PPT is important since it can be used to characterize the performance of a thruster. It is also required in order to accurately gauge how a thruster may affect a host satellite. Unfortunately, the transient nature of PPT discharges and insufficient knowledge regarding the discharge and acceleration processes has posed some challenges. Unlike electrostatic thrusters such as Hall thrusters and ion engines, the plasma produced by a PPT is usually composed of multiple elemental species with different ionization levels. Exhaust velocity measurements of different PPTs have also resulted in values in a wide range from 5 to 60 km/s. To further our understanding regarding the fundamental physics behind a PPT, we will present here our results from direct measurements of the acceleration and expansion of the PPT plasma both between the electrodes and in the exhaust plume outside the thruster. For the inter-electrode space, a novel measurement method using a multi-segmented anode was used to obtain data regarding inter-electrode plasma acceleration. These results were compared with time-of-flight measurements using a micro-magnetic probe. For the downstream exhaust plume outside the thruster, time-of-flight measurements were made using Langmuir and Faraday probes. We will also pose a hypothesis to explain why an extremely wide range of exhaust velocity measurements have been reported in the literature. The results are expected to further our understanding regarding PPT plasma acceleration and expansion. They will be useful as a reference to improve the accuracy of future PPT simulations.

---

<sup>1</sup> Associate Professor, School of Aerospace Engineering, Beijing Institute of Technology, wling@bit.edu.cn (corresponding author).

<sup>2</sup> Ph.D. candidate, School of Astronautics, Beihang University.

<sup>3</sup> Professor, School of Astronautics, Beihang University.

## Nomenclature

$d$	=	distance from exit plane
$\Delta t$	=	time difference between discharge onset and signal collection
$t$	=	time
$t_1$	=	time of discharge onset
$t_2$	=	time that a signal is collected
$I_d$	=	discharge current
$I_p$	=	probe current (ion saturation current)
$V_d$	=	discharge voltage

## I. Introduction

Pulsed plasma thrusters (PPTs) are a type of electric propulsion that are highly suitable for small satellites in the kilogram weight range, especially with the recent discovery of a new non-volatile liquid propellant.<sup>1-5</sup> Their operation is triggered by a spark plug, which results in a pulsed operation mode with each pulse being in the order of microseconds. In each discharge, energy stored in a capacitor is released and ablates propellant through the production of a discharge arc.<sup>1-3</sup> This results in a plasma plume that is conventionally thought to be accelerated downstream between the electrodes due to the Lorentz force and ejected at a final exhaust velocity to provide thrust. While the structural design of PPTs is relatively simple, complex phenomena are at play behind every  $\mu\text{s}$ -order long discharge. Fundamental information regarding PPT plasma acceleration is important as it can be used to both characterize the performance of a thruster (e.g., through the specific impulse) and to support the development of more accurate simulation models. It is also important to accurately determine the exhaust velocity to understand plume interactions with the rest of the spacecraft that a thruster is installed on. Unfortunately, the transient nature of PPT discharges and insufficient knowledge regarding the discharge and acceleration processes has posed some challenges. The inter-electrode plasma velocity can be measured using time-of-flight (TOF) methods with micro-magnetic probes, but this is highly sensitive to plasma conditions. The exhaust velocity of PPTs has also previously been estimated to be in a wide range from 5 to 60 km/s.<sup>6-14</sup> Several measurement methods have been used, including high-speed cameras,<sup>6,7</sup> Doppler shift methods,<sup>8,9</sup> time-of-flight (TOF) methods, etc. Occasional discrepancies have also been observed that hint at a non-constant ion velocity in the exhaust plume.<sup>8,11,15</sup> To further our understanding regarding the fundamental processes behind the operation of a PPT, we present here our results from direct measurements of the acceleration and expansion of the PPT plasma both between the electrodes and in the exhaust plume outside the thruster. A novel measurement method is used to obtain data regarding inter-electrode plasma acceleration. TOF measurements were performed in the exhaust plume at multiple downstream distances. We will also pose a hypothesis to explain why an extremely wide range of exhaust velocity measurements have been previously reported.

## II. Methods

### A. Pulsed plasma thruster and vacuum system

The experimental PPT had an oil capacitor rated for a maximum voltage of 2 kV with a capacitance of 10  $\mu\text{F}$ . This corresponds to a maximum discharge energy of 20 J. The electrode length and spacing was 15 and 20 mm, respectively. A side view of a single pulse discharge is shown in Fig. 1. An example of the discharge voltage and current of a single discharge from the PPT is shown in Fig. 2.

The data recorder was a Tektronix DPO3014. The discharge currents were measured using a Tektronix TCP0030A and a Rogowski coil with a calibrated sensitivity of  $9.75 \times 10^{-4}$  V/A; the discharge voltages were measured using a Tektronix P5201. Unless specified, all experiments were conducted in a vacuum chamber with a diameter of 0.8 m and a length of 1.8 m. This will be referred to as the “small vacuum chamber”. For exhaust plume measurements at greater distances, a larger vacuum chamber (referred to as the “large vacuum chamber”) with a diameter of 3 m

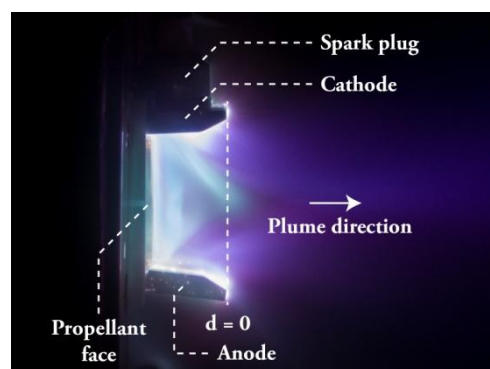


Figure 1. Side-view of a single pulse discharge.

and a length of 5 m was used. Both chambers were used at a base pressure in the order of  $10^{-3}$  Pa before experiments.

## B. Inter-electrode measurements

### 1. Micro-magnetic probe

The magnetic field strength at any point within the space between the electrodes of a PPT (the inter-electrode space) is related to the strength and distribution of the current, with spatial variations in the magnetic field indicating the acting position of the electromagnetic force.<sup>16</sup> The micro-magnetic probe used here was able to be extended within the inter-electrode space. It was constructed using 40 turns of enamel-insulated copper wire around a core holder with a diameter of 2.5 mm. The entire construct was covered with a glass shell with a diameter of less than 3 mm. The probe was located in the center between the electrodes at varying downstream distances. The recorded signals could then be used for TOF measurements to estimate the inter-electrode TOF velocity of the plasma as a function of the downstream distance.

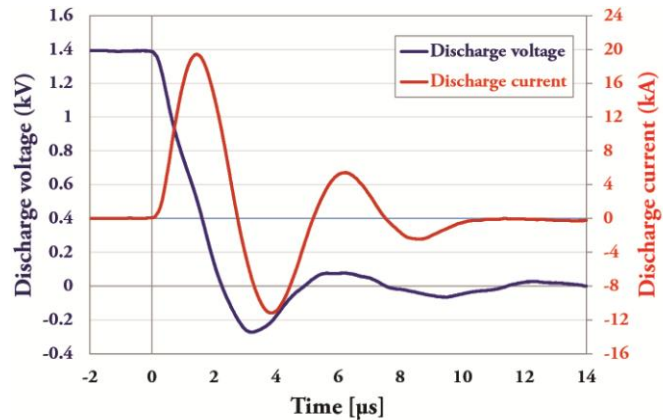


**Figure 2. Discharge voltage and current for an initial discharge voltage of 1.4 kV (9.8 J).**

### 2. Multi-segmented anode

The multi-segmented anode is a novel configuration that divides the anode into 4 segments, with each segment being insulated from the other segments, as shown in Fig. 3. The conducting segments were made of copper while the insulating segments were ceramic. The main anode and a conducting segment were connected to the capacitor. The main anode is identified as  $1^{st}$ , with the downstream segments being  $2^{nd}$ ,  $3^{rd}$ , and  $4^{th}$ . The main anode had a width of 3 mm while the other segments had widths of 2 mm. After the main discharge of the PPT generates a cloud of plasma, the plasma moves downstream and passes over the conducting segments. This results in current flow through the plasma to the segment. A Rogowski coil was used to measure this downstream segment current. This was then compared with the simultaneously measured main discharge current.

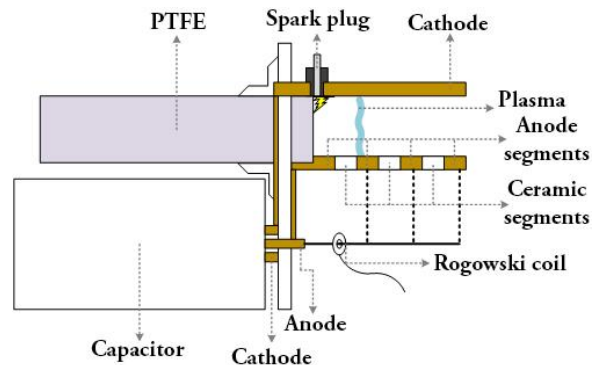


**Figure 3. A schematic of the experimental PPT equipped with a multi-segmented anode. Only one of the electrical connections indicated with dotted lines was connected at a time.**

The time delay between the peak of the downstream segment current in relation to the peak of the main discharge current can be used to identify downstream plasma TOF velocity within the inter-electrode space.

## C. Exhaust plume measurements

### 1. Faraday probe

The Faraday probe used in the experiments was a nude Faraday probe with no applied bias voltage. The probe had a tungsten collector and the diameter of the probe was 4 mm. By locating the probe at various downstream distances along the central horizontal plane of the PPT, the probe was able to collect both electrons and ions upon their arrival. The arrival of electrons results in an almost instantaneous negative signal while the delayed arrival of ions results in an increasing positive charge and a distinct positive slope in the probe signal. This arrival time could be used to calculate the in-plume TOF velocities of the leading edge ions.

## 2. Langmuir probe

The Langmuir probe used here was a triple probe with wire diameters, spacings, and exposed lengths of 2, 7, and 4.5 mm, respectively. The triple Langmuir probe is usually used for determining plasma parameters such as the electron temperature and density.<sup>11,15,17</sup> While there are three exposed wires on a triple probe, the two of interest here are biased with an applied voltage to repel electrons and are used to record the ion saturation current. Hence, the velocity of the leading edge of ions can be estimated by simply using the time difference between discharge initiation and the initial onset of a signal recorded by the probe. A bias voltage of 74 V was used here and the selected bias voltage exhibited stable results.

## III. Results and Discussion

### D. Inter-electrode measurements

The recorded magnetic field strength over time as a function of downstream distance is shown in Fig. 4. It is clear that with increasing downstream distance, the recorded time of the peak magnetic field strength is delayed. This time difference can be used to estimate the local TOF velocities of the inter-electrode plasma. The estimated TOF velocities based on the average peak latencies is shown in Table 1.

**Table 1. TOF velocities from micro-magnetic probe data.**

	Peak latency ( $\mu\text{s}$ )	TOF velocity $v$ (km/s)
2 – 6 mm	0.186	21.5
2 – 10 mm	0.38	21.9
2 – 14 mm	0.52	23.1
Average	-	21.9

This data shows that at just 6 mm from the propellant surface, the inter-electrode plasma has already been accelerated to over 20 km/s, very close to its final exit velocity. While the micro-magnetic probe data allows us to obtain estimates of the inter-electrode velocities, the data is highly susceptible to discharge noise due to the probe being located within the inter-electrode space.

On the other hand, the non-dimensionalized discharge currents for the main discharge and downstream segments are shown in Fig. 5. The phase change due to downstream location is extremely repeatable and the data is far less susceptible to discharge noise. This gives us extremely repeatable and consistent data. Similar with the micro-magnetic probe data, the phase lag can be used to estimate the propagation speed of the plasma between the electrodes. This data is shown in Table 2.

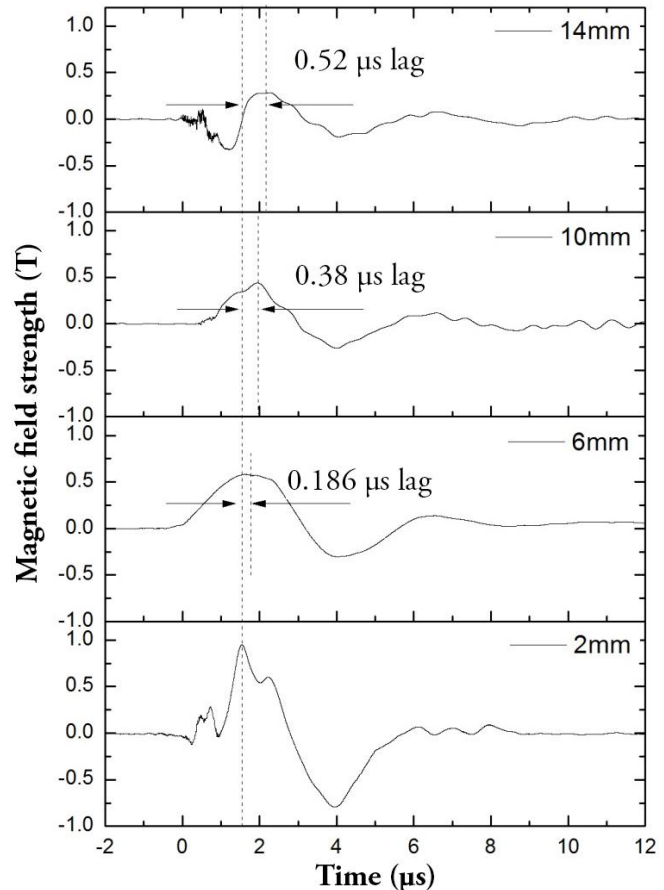


**Figure 4. Recorded magnetic field strengths along the middle plane between the electrodes for downstream distances of 2, 6, 10, and 14 mm.**

**Table 2. TOF velocities using the multi-segmented anode method.**

Segment	Distance to propellant surface (mm)	Peak latency ( $\mu\text{s}$ )	TOF velocity (km/s)
2 <sup>nd</sup>	5	0.2	25.0
3 <sup>rd</sup>	9	0.31	29.0
4 <sup>th</sup>	13	0.46	28.3

As with the micro-magnetic probe data, we can see that over a short distance from the propellant surface, the plasma is already accelerated significantly to velocities of over 20 km/s. This suggests that acceleration within the inter-electrode space largely occurs very near to the propellant surface, possibly due to the significant discharge current carried in the discharge arc. As the discharge arc does not migrate downstream significantly,<sup>6</sup> the Lorentz force acceleration further downstream will be largely dependent on the current-carrying capacity of the plasma itself.

The similarity in the recorded inter-electrode velocities between the multi-segmented anode method and the micro-magnetic TOF method verifies that the novel multi-segmented anode can be used to obtain TOF velocities within the inter-electrode space that are less susceptible to discharge noise. However, it must be noted that while the micro-magnetic probe records data for a given point within the inter-electrode space, the data from a multi-segmented anode is indicative of global plasma conditions as the current must pass through all horizontal planes of the plasma before reaching the anode.

### E. Exhaust plume measurements

An example of the probe signal recorded by a downstream Faraday probe is shown in Fig. 6. It shows that there is an almost immediate build-up of negative charge after a discharge. This is due to the greater velocity of electrons compared to ions. As the ions arrive, there is a prominent reversal in the negative build-up. By comparing the arrival time of the ions with the initial discharge time, we are able to obtain an elapsed time and calculate a TOF velocity.

Similar to the Faraday probe data, an example of the ion saturation current recorded by a downstream triple Langmuir probe is shown in Fig. 7. Since there is a sheath that repels electrons, there is no build-up of negative charge and the arrival of ions is simply indicated by the onset of the recorded ion saturation current. Compared with a Faraday probe, this data is much less susceptible to noise. As a consequence, it is also much more repeatable.

The TOF velocities determined using the Faraday and triple Langmuir probes are shown in Fig. 8 over various downstream distances. It must be noted that previous studies have only used fixed downstream distances or a limited distance range, with

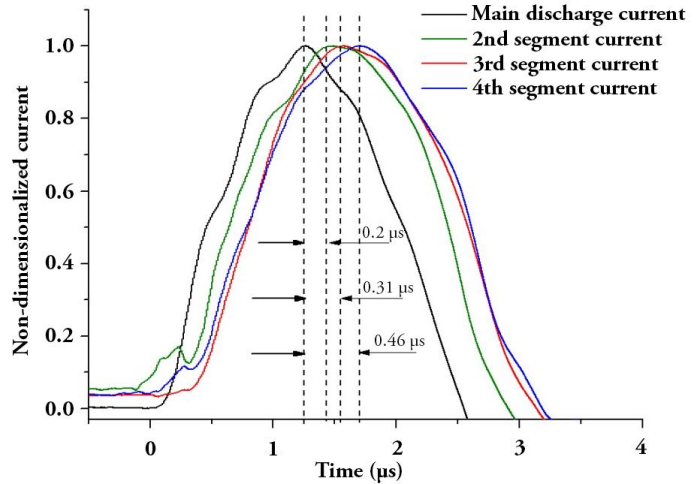


**Figure 5. Non-dimensionalized discharge currents associated with the main discharge current and the 2<sup>nd</sup> to 4<sup>th</sup> downstream segments.**

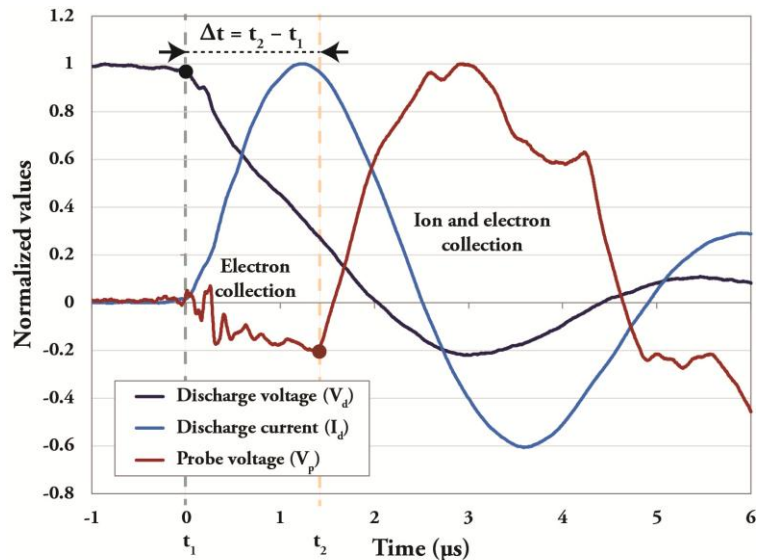


**Figure 6. Example of Faraday probe signal.**

the implicit assumption being that the ions do not accelerate once expelled from the thruster. On the contrary, the data in Fig. 8 shows that there is significant in-plume acceleration of the leading edge of ions. This behavior was observed using both Faraday and triple Langmuir probes and with different vacuum chamber sizes. The difference in the recorded velocities between the Faraday probe and the Langmuir probe can probably be attributed to both discharge noise and the larger collection area of the Faraday probe; the Faraday probe data is susceptible to noise and can vary significantly between discharges. There is also a slight divergence in the small chamber Langmuir probe data at greater distances, possibly due to wall interaction effects.

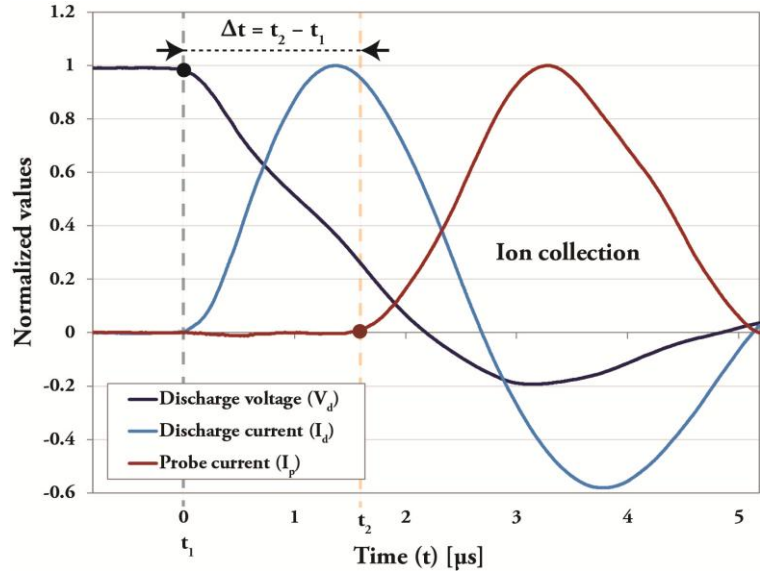


Figure 7. Example of Langmuir probe signal.

While an assumption of there being no in-plume ion acceleration may be true for electrostatic thrusters such as Hall thrusters that emit a uniform composition of an ionized elemental propellant (e.g., xenon), the exhaust plume of a PPT contains electrons and a mixture of ion species with different ionization levels that are formed together during the discharge process.<sup>6,8,10</sup> It is reasonable to expect these components to experience different acceleration forces, resulting in a quasi-neutral plasma plume. In particular, the electrons exhibit a far greater velocity than the ions, as indicated by the build-up of negative charge recorded by the Faraday probe. This temporarily leaves behind a positively charged population of ions. Therefore, it is probable that a form of ambipolar diffusion may act during the expansion of the plasma plume to accelerate the ions outside of the thruster.<sup>18,19</sup> We can expect the fast light-weight electrons to be well-constrained along the centerline due to the self-induced magnetic field of the PPT. This means that off-centerline ions should not exhibit such an acceleration phenomenon, as suggested by some of the results from Gatsonis et al.<sup>17</sup>

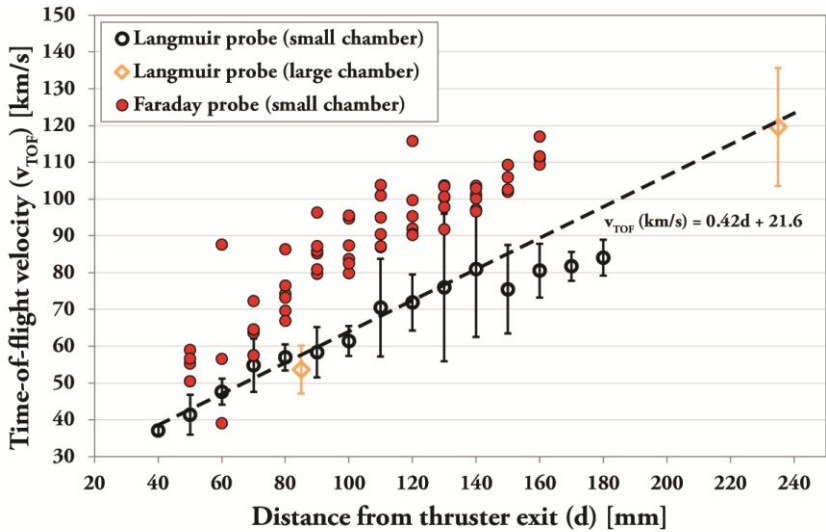


Figure 8. Time-of-flight velocities. The Faraday probe data shows preliminary data. The error bars show 2 standard deviations.

Interestingly, the TOF velocity at the closest exhaust plume probe distance was almost 40 km/s (at a distance of  $40 + 15 = 55$  mm from the propellant surface). This is higher than the inter-electrode velocities in the order of 20 km/s measured using both a micro-magnetic probe and the multi-segmented anode. However, if the small vacuum chamber triple Langmuir probe data from 40 – 140 mm is fitted with a linear fit and extrapolated to the thruster exit, we obtain a velocity of 21.6 km/s.

The data here can be used to further improve PPT plasma plume simulations as the indicated in-plume ion velocity is far higher than previously measured. It also suggests that there is a significant amount of energy still present in the electrons that is subsequently transferred to the ions during their acceleration outside the thruster; this energy is not being utilized as useful thrust. Future PPT designs may be able to take steps to extract more thrust energy from the

plasma and minimize such plume expansion. While the leading edge ion velocity represents a significant increase in the ion energy (the velocities correspond to several hundred eV), it is currently unclear how the rest of the plume behaves. The significant downstream velocity of ions may also affect other spacecraft components in ways that have not yet been considered. In the future, the use of quadruple Langmuir probes can enable the measurement of the mean ion velocities.<sup>15</sup> Although the entire plasma plume is likely to experience the same acceleration phenomena, a thorough understanding of the complete expansion process still requires further work.

#### IV. Conclusion

We presented here new results into the inter-electrode and in-plume acceleration of plasma for a PPT. Using a new method with a multi-segmented anode that is less prone to discharge noise compared with a micro-magnetic probe, we showed that most of the acceleration of the plasma occurs very close to the propellant surface, with the plasma reaching velocities in the order of 20 km/s within 5 mm. This suggests that most of the Lorentz force acceleration may be due to the discharge current passing through the discharge arc. Further downstream, the plasma will be further from the discharge arc (which moves downstream relatively slowly) with the primary Lorentz force component being dependent on the maximum current that can be carried by the downstream plasma. In the plasma plume, we used TOF measurements with Faraday and triple Langmuir probes to demonstrate the in-plume acceleration of the leading edge ions. We show that the measured exhaust velocity is strongly dependent on the downstream measurement distance. This may have partially resulted in the wide range of exhaust velocities that have previously been reported. It also suggests that some component of the inter-electrode acceleration may be due to the plume expansion phenomenon highlighted here.

#### Acknowledgments

Part of this work was supported by the Australian Government Endeavour Research Fellowship.

#### References

- <sup>1</sup>Burton, R. L., and Turchi, P. J., "Pulsed Plasma Thruster," *Journal of Propulsion and Power*, Vol. 14, No. 5, 1998, pp. 716-735.
- <sup>2</sup>Jahn, R. G., *Physics of Electric Propulsion*, McGraw-Hill, New York, 1968.
- <sup>3</sup>Schönherr, T., "Plasma Acceleration in Ablative Pulsed Plasma Thrusters," *Encyclopedia of Plasma Technology*, edited by J. Shohet, Taylor & Francis, New York, 2016, Vol. 2, pp. 1452-1461.
- <sup>4</sup>Szelecka, A., Kurzyna, J., Daniłko, D., and Barral, S., "Liquid micro pulsed plasma thruster," *Nukleonika*, Vol. 60, 2015, pp. 257-261.
- <sup>5</sup>Ling, W. Y. L., Schönherr, T., and Koizumi, H., "Characteristics of a non-volatile liquid propellant in liquid-fed ablative pulsed plasma thrusters," *Journal of Applied Physics*, Vol. 121, 2017, 073301.
- <sup>6</sup>Koizumi, H., Noji, R., Komurasaki, K., and Arakawa, Y., "Plasma acceleration processes in an ablative pulsed plasma thruster," *Physics of Plasmas*, Vol. 14, 2007, 033506.
- <sup>7</sup>Nawaz, A., and Lau, M., "Plasma Sheet Velocity Measurement Techniques for the Pulsed Plasma Thruster SIMP-LEX," *32nd International Electric Propulsion Conference*, IEPC-2011-248, Wiesbaden, Germany, 2011.
- <sup>8</sup>Thomassen, K. I., and Vondra, R. J., "Exhaust Velocity Studies of a Solid Teflon Pulsed Plasma Thruster," *Journal of Spacecraft and Rockets*, Vol. 9, 1972, pp. 61-64.
- <sup>9</sup>Guman, W., and Begun, M., "Exhaust plume studies of a pulsed plasma thruster," *13th International Electric Propulsion Conference*, San Diego, USA, 1978.
- <sup>10</sup>Markusic, T. E., and Spores, R. A., "Spectroscopic emission measurements of a pulsed plasma thruster plume," *33rd Joint Propulsion Conference and Exhibit*, Joint Propulsion Conferences, AIAA Paper 97-2924, Seattle, USA, 1997.
- <sup>11</sup>Gatsonis, N. A., Eckman, R., Yin, X., Pencil, E. J., and Myers, R. M., "Experimental Investigations and Numerical Modeling of Pulsed Plasma Thruster Plumes," *Journal of Spacecraft and Rockets*, Vol. 38, No. 3, 2001, pp. 454-464.
- <sup>12</sup>Myers, R., Arrington, L., Pencil, E., Carter, J., Heminger, J., and Gatsonis, N., "Pulsed plasma thruster contamination," *32nd Joint Propulsion Conference and Exhibit*, Joint Propulsion Conferences, AIAA Paper 96-2729, Lake Buena Vista, USA, 1996.
- <sup>13</sup>Bushman, S. S. and Burton, R. L., "Heating and Plasma Properties in a Coaxial Gasdynamic Pulsed Plasma Thruster," *Journal of Propulsion and Power*, Vol. 17, No. 5, 2001, pp. 959-966.
- <sup>14</sup>Gatsonis, N. A., Zwahlen, J., Wheelock, A., Pencil, E. J., and Kamhawi, H., "Pulsed Plasma Thruster Plume Investigation Using a Current-Mode Quadruple Probe Method," *Journal of Propulsion and Power*, Vol. 20, No. 2, 2004, pp. 243-254.
- <sup>15</sup>Gatsonis, N. A., Byrne, L. T., Zwahlen, J. C., Pencil, E. J., and Kamhawi, H., "Current-mode triple and quadruple Langmuir probe methods with applications to flowing pulsed plasmas," *IEEE Transactions on Plasma Science*, Vol. 32, No. 5, 2004, pp. 2118-2129.

<sup>16</sup>Lau, M., Manna, S., Herdrich, G., Schönherr, T., and Komurasaki, K., “Investigation of the Plasma Current Density of a Pulsed Plasma Thruster.” *Journal of Propulsion and Power*, Vol. 30, No. 6, 2014, pp. 1459-1470,

<sup>17</sup>Eckman, R., Byrne, L., Gatsonis, N. A., and Pencil, E. J., “Triple Langmuir Probe Measurements in the Plume of a Pulsed Plasma Thruster,” *Journal of Propulsion and Power*, Vol. 17, No. 4, 2001, pp. 762-771.

<sup>18</sup>Longmier, B. W., Bering III, E. A., Carter, M. D., Cassady, L. D., Chancery, W. J., Glover, T. W., Hershkowitz, N., Ilin, A. V., McCaskill, G. E., Olsen, C. S., and Squire, J. P., “Ambipolar ion acceleration in an expanding magnetic nozzle”, *Plasma Sources Science and Technology*, Vol. 20, 2011, 015007.

<sup>19</sup>Keidar, M., and Beilis, I. I., *Plasma Engineering: Applications from Aerospace to Bio- and Nanotechnology*, Academic Press, 2013, p. 136.